Chapter

Brushite: Synthesis, Properties, and Biomedical Applications

Khalil Issa, Abdulaziz Alanazi, Khalid A. Aldhafeeri, Ola Alamer and Mazen Alshaaer

Abstract

In this chapter, besides its biomedical applications, the synthesis and properties of brushite were investigated. Brushite consists of two types of crystals, platy and needle-like, and their formation depends on the pH of the medium during precipitation. Platy crystals are formed in a slightly acidic medium, pH = 5, and needle-like crystals at a higher pH = 6.5–7. In this study, the monoclinic brushite crystals were synthesized using dissolution-precipitation reactions. It is found that the brushite crystal growth occurs mainly along the (020) crystallographic plane. The thermogravimetric analysis confirms the presence of the two structural water molecules, which decompose at a temperature range between 80 and 220°C. Brushite was used in the preparation of tetracalcium phosphate mineral, which is the powder component for calcium phosphate cement (CPC). CPC was subsequently prepared from TTCP and phosphate-based hardening solution. *In vitro* evaluation of the resultant CPC using Hanks' Balanced Salt Solution results in the growth of nanofibrous crystals of Calcium-deficient hydroxyapatite (CDHA) layers on the surfaces of the CPC. The cultured CPC exhibits new connective tissues and throughout the CaP matrix.

Keywords: brushite, hydroxyapatite, tetracalcium phosphates, bioactivity, porosity

1. Introduction

Calcium phosphates (CaP) are one of the most important compounds found in nature [1, 2]. There are many applications for these compounds in various fields, especially agricultural, environmental, and medical applications. CaP are characterized by their wide diversity as it is produced at different temperatures and pH ranges. In addition, the molar ratio of calcium to phosphorous in the precursors plays an important role in the resulting materials. The biochemical characteristics and mineralogical structures of CaP are similar to inorganic constituents of mammals' bones [3, 4]. Because of their excellent biocompatibility, high bioactivity, and low toxicity, CaP are considered as a good candidate for bone tissue engineering applications. The CaP minerals such as hydroxyapatite, brushite, tricalcium phosphates (TCP) are used as precursors for the preparation of bone cements and bio-ceramics [5, 6]. Therefore, these minerals are widely used for biomedical applications such as drug delivery and bone tissue engineering (**Table 1**) [6–9].

CaP belong to the family of apatite. There are several CaP phases, the most ubiquitous being hydroxyapatite [HAp, $Ca_{10}(PO_4)_6(OH)_2$]. Other CaP structures include brushite (DCPD, $CaHPO_4{\cdot}2H_2O$) and tricalcium phosphate

Ca/P ratio	Compound	Formula	Density (g/cm^3)	pH stability range (25°C) [a]
0.5	monocalcium phosphate monohydrate (MCPM)	$Ca(H_2PO_4)_2{\cdot}H_2O$	2.23	0.0–2.0
0.5	monocalcium phosphate anhydrate (MCPA)	$Ca(H_2PO_4)_2$	2.58	[d]
1.0	dicalcium phosphate dihydrate (DCPD, brushite)	$CaHPO_4{\cdot}H_2O$	2.32	2.0–6.0
1.0	dicalcium phosphate anhydrate (DCPA, monetite)	$CaHPO_4$	2.89	[d]
1.0	Calcium pyrophosphate (pyro)	$Ca_2P_2O_7$	_	_
1.33	octacalcium phosphate (OCP)	$Ca_8(HPO_4)_2(PO_4)_4{\cdot}5H_2O$	2.61	5.5–7.0
1.5	α-tricalcium phosphate (α-TCP)	$\alpha\text{-}Ca_3(PO_4)_2$	2.86	[b]
1.5	β-tricalcium phosphate (β-TCP)	$\beta\text{-}Ca_3(PO_4)_2$	3.07	[b]
1.2–2.2	amorphous calcium phosphate (ACP)	$Ca_x(PO_4)y{\cdot}nH_2O$	—	[c]
1.5–1.67	calcium-deficient hydroxyapatite (CDHA)	$Ca_{10-x}(HPO_4)_x(PO_4)_{6-x}(OH)_{2-x}$ $(0 < x < 1)$		6.5–9.5
1.67	hydroxyapatite (HAp)	$Ca_{10}(PO_4)_6(OH)_2$	3.15	9.5–12
2.0	tetracalcium phosphate (TTCP)	$Ca_4(PO_4)_2O$	3.05	[b]

[a] In aqueous solution, [b] These compounds cannot be precipitated from aqueous solutions. [c] Cannot be measured precisely. However, the following values were reported: 25.7 ± 0.1 (pH 7.40), 29.9 ± 0.1 (pH 6.00), and 32.7 ± 0.1 (pH 5.28). [d] Stable at temperatures above 100°C.

Table 1.
List of main phases of CaP [6–9].

(TCP, $Ca_3(PO_4)_2$). Several low- and high-temperature approaches have been reported for synthesizing HAp and brushite (DCPD), while TCP is primarily synthesized using high-temperature methods [6]. The chemical formation of CaP minerals is common in natural systems, although the elucidation of the mechanisms of formation and transformations between the crystal forms of the minerals remains a major challenge. The most thermodynamically stable form, at ambient temperature and pressure, is calcium hydroxyapatite (HAp); however, this does not form readily without a transition phase. Other mineral phases, such as octacalcium phosphate (OCP) and amorphous TCP, are precursor phases that can transform to HAp [10].

Acidic CaP, such as brushite (dicalcium phosphate dehydrate, DCPD), are thermodynamically unstable under pH values greater than 6–7 and thus undergo transformation into more stable CaP. Researchers have also demonstrated that meta-stable brushite (DCPD) may convert to OCP or calcium hydroxyapatite (HAp), and that OCP may convert to hydroxyapatite, depending on the Ca/P ratio and the pH value of the setting reactions [11]. Brushite, a type of CaP that is the most easily synthesized, transforms into monetite (dicalcium phosphate anhydrate, DCPA) at temperatures above 80°C. Monetite (DCPA) is the anhydrous form of brushite (DCPD) and can, like brushite, be crystallized from aqueous solutions, but only when the temperature is above 80°C. At low pH values (<7), monetite is the most stable of the CaP, although the conversion of brushite to monetite is faster when the water is warmer and more acidic [8].

Brushite-based biomaterials are characterized by good bioactivity, and they are bioresorbable and biocompatible. Unlike apatite-based materials, brushite-based

ones are rapidly resorbed in vivo [12]. The bioactivity and biocompatibility of brushite-based biomaterials have been investigated in several compositions, applications, and in vivo [11]. Brushite-based materials are biocompatible with and tolerated by soft tissues and bone in vivo, so that material resorption was shortly followed by the formation of new bone tissues. Histological measurements and experimental studies indicate that brushite-based materials feature good biocompatibility, with no appearance of inflammatory cells [12].

Amorphous calcium phosphate (ACP) is often encountered as a transient phase during the formation of CaP in aqueous systems. Usually, ACP is the first phase that is precipitated from a supersaturated solution prepared by the rapid mixing of solutions containing calcium cations and phosphate anions. The chemical composition of ACP strongly depends on the solution's pH value and the concentrations of calcium and phosphate ions. For example, ACP phases are formed with Ca/P ratios in the range of 1.18:1 (precipitated in a solution with a pH value of 6.6) to 1.53:1 (precipitated in a solution with a pH value of 11.7), although ratios of up to 2.5:1 have also been encountered [8]. The structure of ACP is still uncertain and it has been reported to be more soluble than brushite [13]. ACP could be stabilized by another chemical compound: e.g., pyrophosphate ($P_2O_7^{4-}$) retards the conversion of ACP to apatite. Finally, ACP is characterized by its relatively high solubility and ability to obtain a substantial release of Ca^{2+} and PO_4 ions [12].

This chapter aims to synthesis brushite as one of the most common CaP. The microstructural and thermal properties of this mineral are characterized and discussed. After that, the thermochemical transformation of brushite was investigated. The resultant compound is used as precursors for bone cement. Finally, biomineralization and the bioactivity, and biomineralization of calcium phosphate cement (CPC) are studied *in vitro*.

2. Synthesis of brushite ($CaHPO_4{\cdot}2H_2O$)

The typical method synthesis of the brushite powder was performed at ambient according to the following equation:

$$Ca(NO_3)_2 + Na_2HPO_4 \rightarrow CaHPO_4{\cdot}2H_2O + 2NaNO_3 \quad (1)$$

Two solutions were prepared for the synthesis of brushite. The first solution is prepared by dissolving 0.5 mol of $Na_2HPO_4{\cdot}2H_2O$ in 1 L of distilled water, and the second solution is a result of dissolving 0.5 mol of $Ca(NO_3).6H_2O$ in 1 L of distilled water. After preparing the solutions, 200 ml of the $Ca(NO_3)_2$ was added dropwise using a glass funnel with a glass stopcock (flow rate is 2 ml/min) to the $Na_2HPO_4{\cdot}2H_2O$ solution while stirring and adjusting the pH between 6 and 6.5 using ammonia solution (25%, Labochemie, India). Afterward, the resultant solution with precipitates was stirred (400 rpm) at ambient conditions for 1 hour to ensure a homogeneous mixture. The precipitate was vacuum filtered using a qualitative filter paper via a Buchner funnel, washed three times with de-ionized water and another three times with ethanol to reduce the possibility of agglomeration [14, 15], after which it was placed upon a watch glass and dried at 40°C overnight in a drying-oven. After the formation of the precipitate, some of the powder was washed with distilled water, then dried using ethanol at 40°C for a week. The major steps of the experimental design are reported in **Figure 1**.

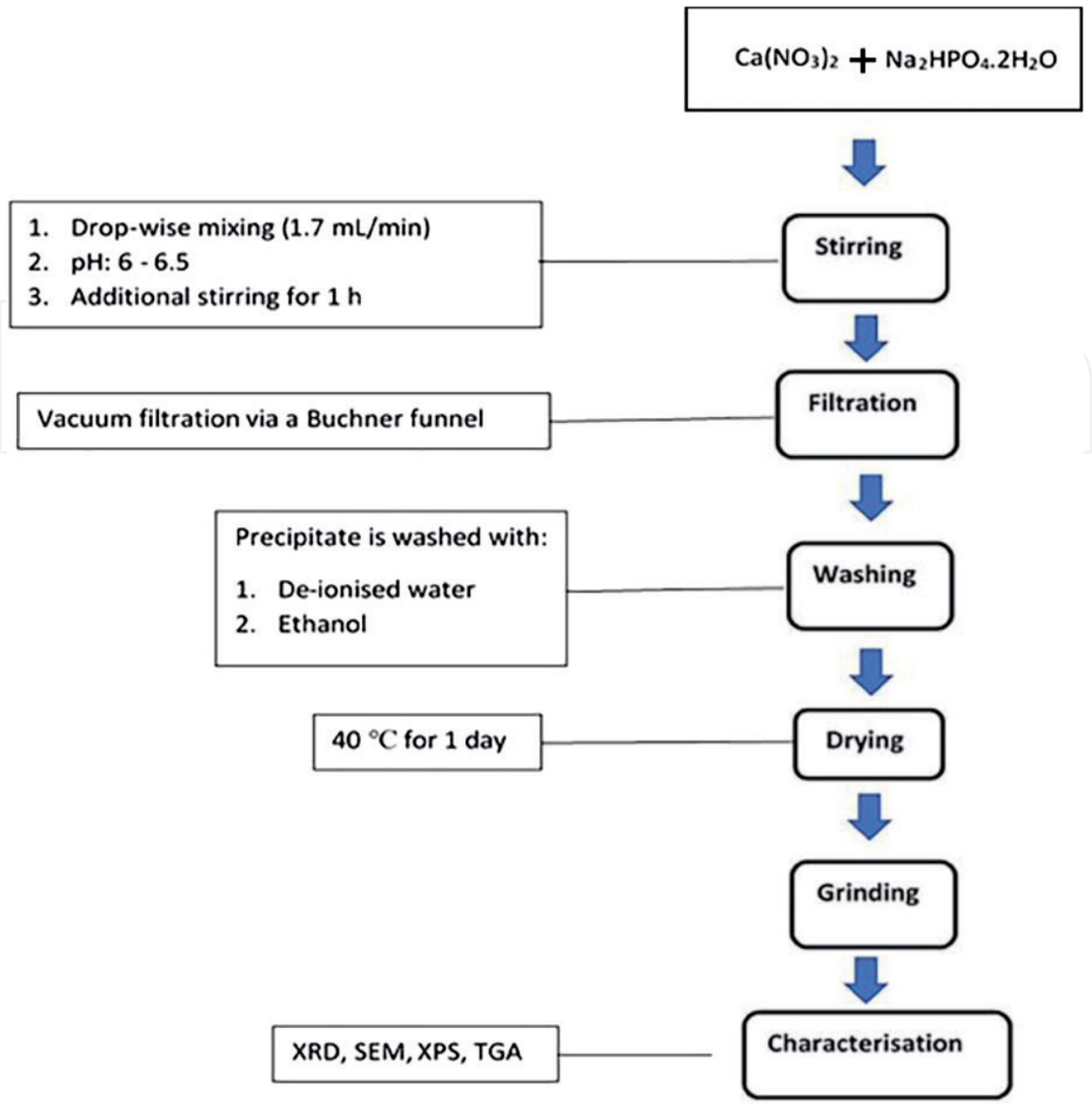

Figure 1.
preparation of brushite [16].

3. Crystal morphology of brushite

Two morphologies of brushite crystal layers are reported in our previous work [17]. These brushite crystals consist of [2] platy particles (**Figure 2A**) and a continuous needle-like (**Figure 2B**) dendritic network [18]. The plate-like brushite crystals mostly formed in parallelogram shapes stacked in multiple layers. Their dimensions ranged from 1 μm to a few micrometers, in two directions. The thickness of the platy crystals is measured in the nano-scale. The needle-like brushite particles appeared to have a dendritic network structure. The total length of the crystal is around 40 μm. The EDS measurements (**Figure 2C**) showed that the needle-like brushite crystals are composed of, by atomic percentage: O (76.46%), Ca (12.04%), and P (10.95%). The fact that the percentages of P and Ca are nearly equal and is in good agreement with the theoretical Ca/P atomic percentages of brushite [19, 20]. The brushite morphology depends on the pH of the solution during the precipitation; at acidic pH, around 5, platy crystals of brushite are formed (**Figure 2A**), whereas needle-like (**Figure 2B**) ones are predominant at a higher pH [2].

SEM images of the brushite crystals are shown in **Figure 3**. These plate-like crystals are obtained according to the experimental procedure as reported in **Figure 1**.

DOI: http://dx.doi.org/10.5772/intechopen.102007

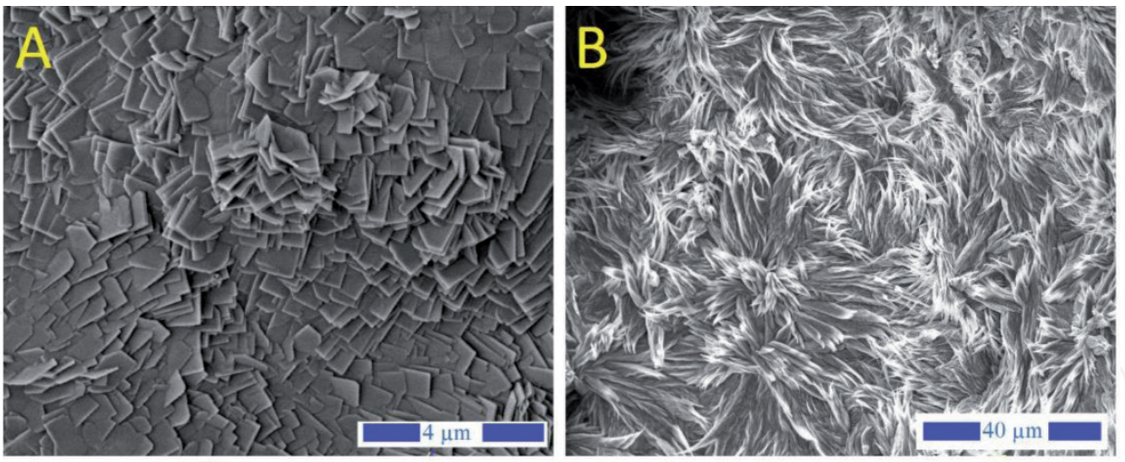

C

El	AN	Series	unn. C [wt.%]	norm. C [wt.%]	Atom. C [at.%]	Error [%]
O	8	K-series	58.66	59.45	76.46	7.0
Na	11	K-series	0.61	0.62	0.55	0.1
P	15	K-series	16.26	16.48	10.95	0.6
Ca	20	K-series	23.15	23.46	12.04	0.8

Figure 2.
(A) crystal morphologies of brushite; platy structure, (B) needle-like structure, and (C) EDS analysis [17].

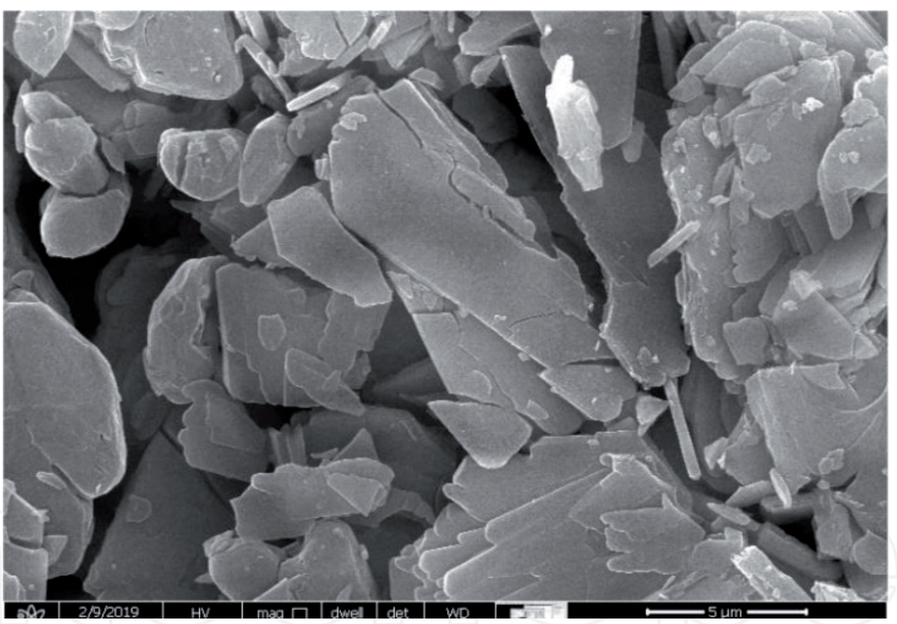

Figure 3.
SEM image of monoclinic brushite crystals, see ***Figure 1*** *(preparation procedure).*

It is known that the morphology of brushite is characterized by a plate-like or needle-like structure, depending on the solution pH used [11, 13]. The plate-like crystals are thin (~400 nm), while their width and elongation are approximately 10 and 20 µm, respectively, values similar to those reported in other studies [21].

The XRD patterns of brushite, as well as the patterns of standard brushite, are shown in **Figure 4**. The mineralogy of the powder confirms that this precipitate produced after mixing $NaH_2PO_4{\cdot}2H_2O$ and $Ca(NO_3)_2{\cdot}4H_2O$ solutions with a Ca:P molar ratio 1:1 (**Figure 1**) is pure brushite, while its crystals grow after nucleation in proportion to the three major planes, namely, (020), (121-), and (141). All peaks of the powder pattern denote the brushite's monoclinic structure [16], while the peak at 11.7° 2-Theta indicates that the crystal growth takes place primarily along the (020) crystallographic plane. Rietveld refined unit cell parameters for brushite are presented in **Table 2**.

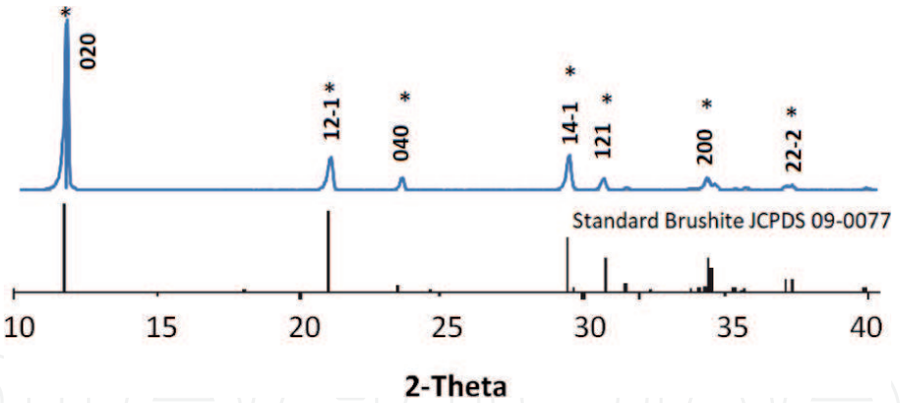

Figure 4.
*XRD patterns of brushite (synthesis details are shown in **Figure 1**) [16].*

wt%	a(Å)	b(Å)	c(Å)	(βo)	V(Å3)
100.0	5.8145	15.1693	6.2399	116.392	492.83

**Standard deviation varied between 0.001 and 0.005 for all samples.*

Table 2.
*Refined unit cell parameters for brushite from XRD data using the Rietveld approach.**

4. Thermal properties of brushite

The results of the TG analysis for the brushite are reported in **Figure 5**. Brushite is considered as a water-bearing phosphate mineral [2] and its crystal structure contains compact sheets consisting of parallel chains in which Ca ions are coordinated by six phosphate ions and two oxygen atoms belonging to the water molecules [22].

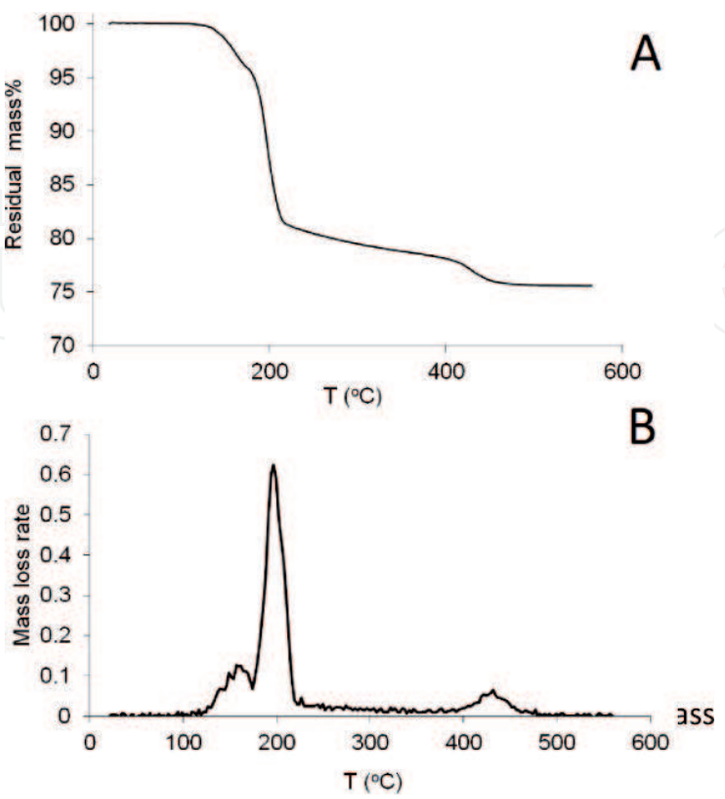

Figure 5.
TGA of brushite: (A) cumulative mass loss, and (B) mass loss rate.

Brushite contains two water molecules in its lattice and adsorbed water molecules on its surface, as indicated by the presence of two sharp peaks of mass loss during heating between 80 and 220°C (**Figure 5A**) [2, 23]. Part of the chemically-bound water is released during the transformation of brushite to monetite, $CaHPO_4$, at ~220°C [17], and later to calcium pyrophosphate, $Ca_2P_2O_7$, at ~400°C [24]. Pyrophosphates are decomposed at higher temperatures of 750–800°C (**Figure 5B**) [8, 25]. The heating of pure brushite to 600°C results in a mass loss of approximately 25%wt, while the theoretical mass loss for the dehydration of brushite is 20.93%wt [1].

Dehydration of brushite over the temperature range 110–215°C takes place according to Eq. (2) and normally results in a weight loss of about 19%wt, while the formation of calcium pyrophosphate is accomplished by Eq. (3) a

$$CaHPO_4 \cdot 2H_2O \rightarrow CaHPO_4 + 2H_2O \tag{2}$$

$$2CaHPO_4 \rightarrow Ca_2P_2O_7 + H_2O \tag{3}$$

Figure 5B shows the rate of mass loss as a function of heating temperature for brushite. More specifically, **Figure 5B** shows the dehydration peaks corresponding to the two water molecules of brushite [26, 27].

5. Calcium phosphate cement (CPC)

Brushite is used to prepare the powder component, tetracalcium phosphate (TTCP), of the CPC. Brushite was calcined at 500°C and transformed into a more stable phase; calcium pyrophosphate ($Ca_2P_2O_7$). Afterward, calcium pyrophosphate and calcium carbonate were mixed with a Ca/P molar ratio of 1.9 [5]. These two compounds were mixed in ethanol for 10 h. Then the resultant mixture was dried at 105°C for 24 h and then crushed. The mixture was heated at 1500°C for 4 h quenching to room temperature, see **Figure 7**. The resultant powder (TTCP) was ground into a fine powder [5]. The general equation TTCP synthesis is as follows:

$$CaHPO_4 \cdot 2H_2O + 2CaCO_3 \left(1500°C \text{ for } 3h\right) \rightarrow Ca_4\left(PO_4\right)_2O + 2CO_2 \tag{4}$$

Mannitol, sizes vary from 100 to 400 μm, was added to the TTCP with the weight ratio of 0.5. Diammonium hydrogen phosphate solution with a concentration of 33.3 wt% was mixed with TTCP-mannitol mixture, with the weight ratio of O.34 mL (solution)/g (TTCP). After mixing the CPC components for 2 min, the paste was packed in a polycarbonate mold which has an opening of 10 × 10 mm under a pressure of ~1 MPa at 37°C. The hardened samples were then demolded and immersed in Hanks' physiological solution at 37°C for 1 day [28, 29]. The composition of Hanks' physiological solution is reported in **Table 3**.

After mixing the two components of CPC, TTCP, and the hardening solution, TTCP hydrolyses through a dissolution-precipitation reactions resulting in the formation of layers of Ca-deficient hydroxyapatite (CDHA) crystals, which are similar to the mineral component of the bone from (**Figure 6**). This hydrolysis process occurs during the setting reactions, which is confirmed by XRD and SEM (**Figures 7** and **8**). These CDH layers are characterized by wide range distribution of rod-like crystals [30].

The CPC was synthesized for *in vitro* cultivation [5, 31, 32]. Mesenchymal stem cells (MSCs) were seeded on the CPC porous matrix in presence of an osteogenic

Component	Concentration
NaCl (mw: 58.44 g/mol)	0.14 M
KCl (mw: 74.55 g/mol)	0.005 M
$CaCl_2$ (mw: 110.98 g/mol)	0.001 M
$MgSO_4.7H_2O$ (mw: 246.47 g/mol)	0.0004 M
$MgCl_2.6H_2O$ (mw: 203.303 g/mol)	0.0005 M
$Na_2HPO_4.2H_2O$ (mw: 177.99 g/mol)	0.0003 M
KH_2PO_4 (mw: 136.086 g/mol)	0.0004 M
D-Glucose (Dextrose) (mw: 180.156 g/mol)	0.006 M
$NaHCO_3$ (mw: 84.01 g/mol)	0.004 M

Table 3.
Composition of Hanks' physiological solution.

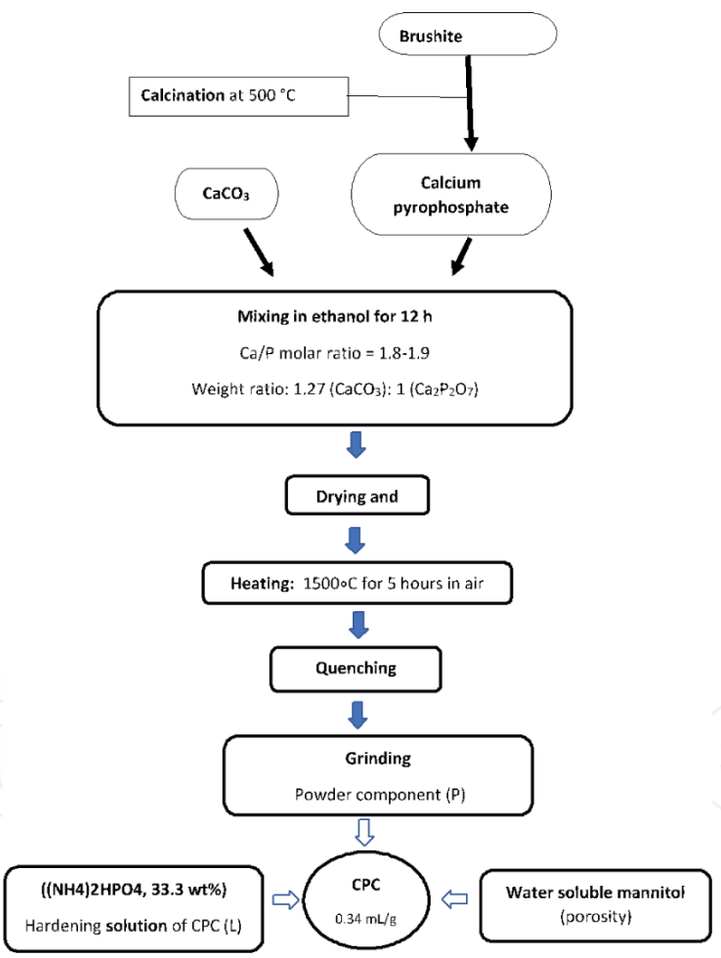

Figure 6.
Schematic diagram of CPC preparation.

medium for 21 days [5, 12]. As a result of *in vitro* cultivation, mineralized nodules were formed in the constructs. The seeded cells grow and their sizes increase from 5 μm to around 50 μm. The growing cells adhered to the CPC matrix and developed cytoplasmic extension as reported in **Figure 8**.

A thick layer of nano fibrous CDH crystals covers the surfaces of the CPC matrix (**Figure 7B**). The cultured CPC exhibits new connective tissues and throughout the CaP matrix (**Figure 8**). The CPC matrix contains bioactive CDH with both Ca and P,

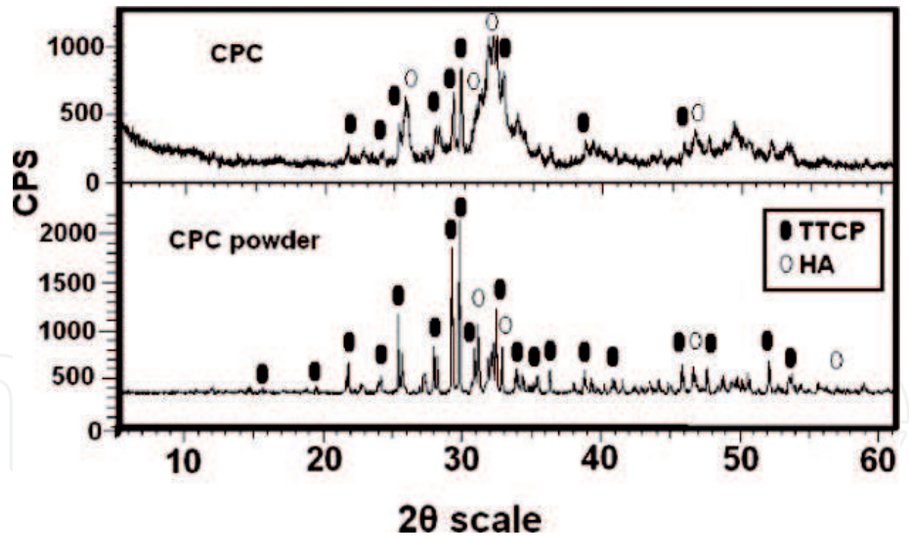

Figure 7.
XRD patterns of CPC and CPC powder [5].

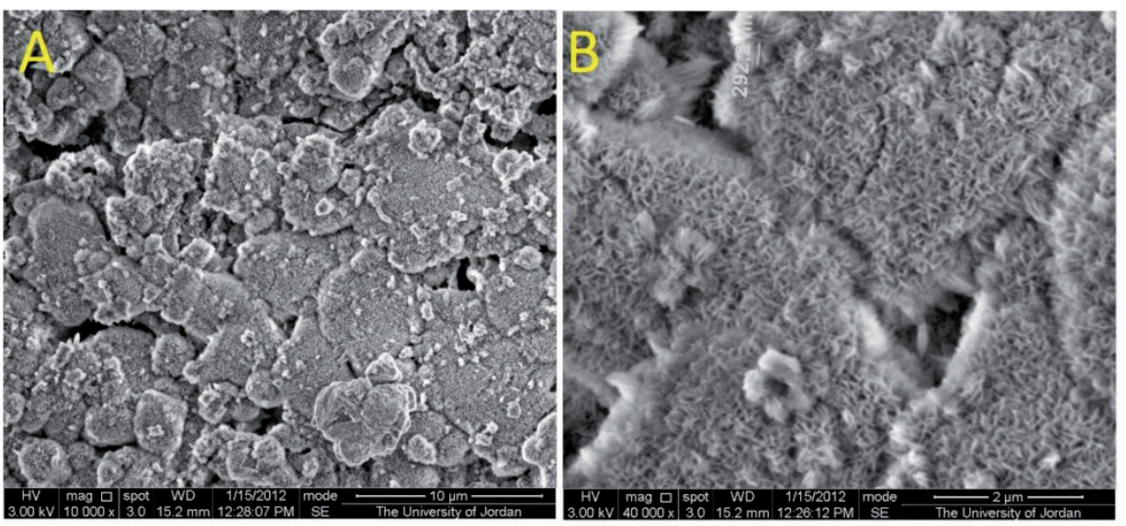

Figure 8.
Growth of thick Ca-deficient hydroxyapatite (CDHA) layer on the surface of the CaP matrix.

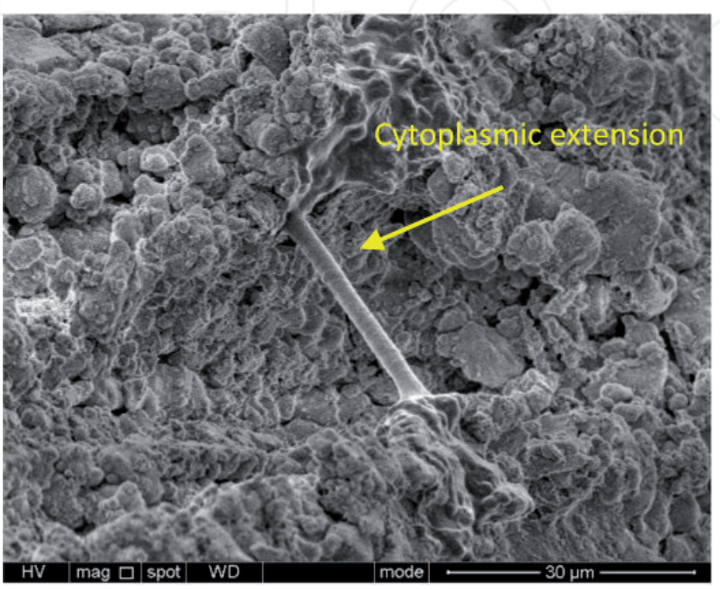

Figure 9.
SEM image of the surface of CPC after MSCs culturing for 21 days.

therefore, this matrix provides the appropriate environment for MSCs growth and osteogenic differentiation (**Figure 9**) [33].

6. Conclusions

Brushite crystals consist of platy and needle-like crystals. It is found that the pH of the solution during the precipitation of brushite plays the main role in determining the shape of the crystals. Usually at a relatively low pH, around 5, platy crystals are formed, while at a higher pH, around ph = 6.5, needle-like crystals are precipitated. In this study, brushite crystals with a monoclinic structure were synthesized using calcium and phosphate salts. The brushite crystal growth occurs mainly along the (020) crystallographic plane. Brushite crystal is characterized by the presence of two structural water molecules. These two molecules are released at a temperature range between 80°C and 220°C to form monetite minerals.

In this chapter, brushite is used as a precursor to synthesize TTCP, the powder components of CPC. As a result of the solid reactions between brushite and calcium carbonate, at high temperature, 1500°C, a new CaP phase is called TTCP. This powder reacts with the phosphate-based solution at 37°C to form CDHA. Immersing this CPC in Hanks' Balanced Salt Solution results in the growth of nanofibrous crystals of CDHA layers on the surfaces of the CPC. The cultured CPC exhibits new connective tissues and throughout the CaP matrix. The CPC matrix contains bioactive CDH with both Ca and P, therefore this matrix provides an appropriate environment for MSCs growth and osteogenic differentiation.

Bioactive features of brushite-based materials affect cell adhesion, proliferation, and new bone formation. Bioactivity can be altered and controlled by the crystal structure and physical property of the scaffold. Bioactive characteristics are different depending on the produced type of CaP phases such as HAP, TCP, and ACP. These different bioactive characteristics are caused by the differences in Ca/P ratio, crystal structure, stability, and solubility. As mentioned above, brushite is often used with other CaP to control and improve their chemical, biological, and physical properties. Various applications have been exploited to actively utilize the bioactive features of brushite in bone regeneration.

DOI: http://dx.doi.org/10.5772/intechopen.102007

Author details

Khalil Issa[1*], Abdulaziz Alanazi[2], Khalid A. Aldhafeeri[2], Ola Alamer[3] and Mazen Alshaaer[2,4]

1 Faculty of Medicine and Health Sciences, Orthopedics Unit, An-Najah National University, Nablus, Palestine

2 Department of Physics, College of Science and Humanities in Al-Kharj, Prince Sattam Bin Abdulaziz University, Al-Kharj, Saudi Arabia

3 Faculty of Applied Science, Department of Physics, Umm Al-Qura University, Makkah, Saudi Arabia

4 GeoBioTec Research Center, University of Aveiro, Campus de Santiago, Aveiro, Portugal

*Address all correspondence to: k.issa@najah.edu

References

[1] Kim Y, Lee SY, Roh Y, Lee J, Kim J, Lee Y, et al. Optimizing calcium phosphates by the control of pH and temperature via wet precipitation. Journal of Nanoscience and Nanotechnology. 2015;**15**(12):10008-10016

[2] Suryawanshi VB, Chaudhari RT. Growth and characterization of agar gel grown brushite crystals. Indian Journal of Materials Science. 2014;**2014**:1-6

[3] Alshaaer M, Kailani MH, Ababneh N, Mallouh SAA, Sweileh B, Awidi A. Fabrication of porous bioceramics for bone tissue applications using luffa cylindrical fibres (LCF) as template. Processing and Application of Ceramics. 2017;**11**(1):13-20

[4] Radwan NH, Nasr M, Ishak RA, Abdeltawa NF, Awad GA. Chitosan-calcium phosphate composite scaffolds for control of postoperative osteomyelitis: Fabrication, characterization, and in vitro–in vivo evaluation. Carbohydrate Polymers. 2020;**244**:116482

[5] Alshaaer M, Kailani MH, Jafar H, Ababneh N, Awidi A. Physicochemical and microstructural characterization of injectable load-bearing calcium phosphate scaffold. Advances in Materials Science and Engineering. 2013;**2013**:8. Article ID: 149261

[6] Khalifehzadeh R, Arami H. Biodegradable calcium phosphate nanoparticles for cancer therapy. Advances in Colloid and Interface Science. 2020;**279**:102157. DOI: 10.1016/j.cis.2020.102157

[7] Shyong Y-J, Chang K-C, Lin F-H. Calcium phosphate particles stimulate exosome secretion from phagocytes for the enhancement of drug delivery. Colloids and Surfaces B: Biointerfaces. 2018;**1711**:391-397

[8] Alshaaer M, Cuypers H, Rahier H, Wastiels J. Production of monetite-based Inorganic phosphate cement (M-IPC) using hydrothermal post curing (HTPC). Cement and Concrete Research. 2011;**41**:30-37

[9] Alshaaer M, Cuypers H, Mosselmans G, Rahier H, Wastiels J. Evaluation of a low temperature hardening inorganic phosphate cement for high-temperature applications. Cement and Concrete Research. 2011;**41**:38-45

[10] Zhang J, Liu W, Schnitzler V, Tancret F, Bouler J-M. Calcium phosphate cements for bone substitution: Chemistry, handling and mechanical properties. Acta Biomaterialia. 2014;**10**:1035-1049

[11] Mert I, Mandel S, Tas AC. Do cell culture solutions transform brushite (CaHP04 2H20) to octacalium phosphate (Ca8(HP04)2(P04)4 5H20)? In: Narayan R, Colombo P, editors. Advances in Bioceramics and Porous Ceramics IV. Hoboken, New Jersey: John Wiley & Sons, Inc; 2011. pp. 79-94

[12] Hurle K, Oliveira J, Reis R, Pina S, Goetz-Neunhoeffer F. Ion-doped brushite cements for bone regeneration. Acta Biomaterialia. 2021;**123**:51-71

[13] Dosen A, Giese RF. Thermal decomposition of brushite, CaHPO4·2H2O to monetite CaHPO4 and the formation of an amorphous phase. American Mineralogist. 2011;**96**(2-3):368-373

[14] Patil SB, Jena A, Bhargava P. Influence of ethanol amount during washing on deagglomeration of co-precipitated calcined nanocrystalline 3YSZ powders. International Journal of Applied Ceramic Technology. 2012. DOI: 10.1111/j.1744-7402.2012.02813.x

[15] Piva RH, Piva DH, Pierri J, Montedo ORK, Morelli MR. Azeotropic

distillation, ethanol washing, and freeze drying on coprecipitated gels for production of high surface area 3Y–TZP and 8YSZ powders: A comparative study. Ceramics International. 2015;**41**:14148-14156

[16] Alshaaer M, Afify A, Moustapha M, Hamad N, Hammouda G, Rocha F. Effects of the full-scale substitution of strontium for calcium on the microstructure of brushite: (CaxSr1–x)HPO4.nH2O system. Clay Minerals. 2020;**55**(4):366-374

[17] Alshaaer M. Microstructural characteristics and long-term stability of wollastonite-based chemically bonded phosphate ceramics. International Journal of Applied Ceramic Technology. 2021;**18**:319-331

[18] Bhojani A, Jethva H, Joshi M. Growth inhibition study of urinary type brushite crystal using potassium dihydrogen citrate solution. AIP Conference Proceedings. 2019;**2115**:030417. DOI: 10.1063/1.5113256

[19] Wu X, Gu J. Inorganic resins composition, their preparation and use thereof. Belgium/Brussels Patent EP 0 861 216 B1. 2000

[20] Mosselmans G, Biesemans M, Willem R, Wastiels J, Leermakers M, Rahier H, et al. Thermal hardening and structure of a phosphorus containing cementitious model material. Journal of Thermal Analysis and Calorimetry. 2007;**88**:723-729

[21] Sayahi M, Santos J, El-Feki H, Charvillat C, Bosc F, Karacan I, et al. Brushite (Ca,M)HPO4, 2H2O doping with bioactive ions (M = Mg2+, Sr2+, Zn2+, Cu2+, and Ag+): A new path to functional biomaterials? Materials Today Chemistry. 2020;**16**:100230. DOI: 10.1016/j.mtchem.2019.100230

[22] G. Girişken and A. C. Taş, Development of biomineralization solutions to facilitate the transformation of brushite (CaHPO4·2H2O) into octacalcium phosphate (Ca8(HPO4) 2(PO4)4·5H2O), In: 15th National Biomedical Engineering Meeting (BIYOMUT), Antalya, Turkey; 2020

[23] Xue Z, Wang Z, Sun A, Huang J, Wu W, Chen M, et al. Rapid construction of polyetheretherketone (PEEK) biological implants incorporated with brushite (CaHPO4·2H2O) and antibiotics for anti-infection and enhanced osseointegration. Materials Science and Engineering: C. 2020;**111**:110782. DOI: 10.1016/j.msec.2020.110782

[24] Alshaaer M, Cuypers H, Rahier H, Wastiels J. Production of monetite-based inorganic phosphate cement (M-IPC) using. Cement and Concrete Research. 2011;**41**:30-37

[25] Frost RL, Palmer SJ. Thermal stability of the 'cave' mineral brushite CaHPO4·2H2O—Mechanism of formation and decomposition. Thermochimica Acta. 2011;**521**(1-2):14-17

[26] Tamimi F, Le Nihouannen D, Eimar H, Sheikh Z, Komarova S, Barralet J. The effect o fautoclaving on the physical and biological properties of dicalcium phosphate dihydrate bioceramics: Brushite vs. monetite. Acta Biomaterialia. 2012;**8**(8):3161-3169

[27] Tortet L, Gavarri JR, Nihoul G. Study of protonic mobility in CaHPO4 2H2O (Brushite) and CaHPO4 (Monetite) by infrared spectroscopy and neutron scattering. Journal of Solid State Chemistry. 1997;**132**:6-16

[28] Luo J, Engqvist H, Persson C. A ready-to-use acidic, brushite-forming calcium phosphate cement. Acta Biomaterialia. 2018;**81**:304-314

[29] Han L, Qi-Zhi Y, Yu-Ying W, Yi-Liang L, Gen-Tao Z. Biomimetic synthesis of struvite with biogenic morphology and implication for

pathological biomineralization. Scientific Reports. 2015;**5**:7718. DOI: 10.1038/srep07718

[30] Ding H, Pan H, Xu X, Tang R. Toward a detailed understanding of magnesium ions on hydroxyapatite crystallization inhibition. Crystal Growth & Design. 2014;**14**(2):763-769

[31] Li H, Yao Q-Z, Wang Y-Y, Li Y-L, Zhou G-T. Biomimetic synthesis of struvite with biogenic morphology and implication for pathological biomineralization. Scientific Reports. 2015;**5**(1):7718

[32] Nosrati H, Le DQS, Zolfaghari RE, Canillas MP, Bünger CE. Nucleation and growth of brushite crystals on the graphene sheets applicable in bone cement. Boletín de la Sociedad Española de Cerámica y Vidrio. 2020. DOI: 10.1016/j.bsecv.2020.05.001

[33] Alshaaer M, Abdel-Fattah E, Saadeddin I, Al Battah F, Issa KI, Saffarini G. The effect of natural fibres template on the chemical and structural properties of Biphasic Calcium Phosphate scaffold. Materials Research Express. 2020;**7**(6):065405. DOI: 10.1088/2053-1591/ab9993